frontiers | Frontiers in Earth Science

TYPE Original Research
PUBLISHED 30 June 2023
DOI 10.3389/feart.2023.1171452

OPEN ACCESS

EDITED BY
Olev Vinn,
University of Tartu, Estonia

REVIEWED BY
Teuntje Hollaar,
University of Exeter, United Kingdom
Abraham Dabengwa,
University of the Witwatersrand, South Africa

*CORRESPONDENCE
Yuan-Qing Wang,
wangyuanqing@ivpp.ac.cn
Xiaoqiang Li,
lixiaoqiang@ivpp.ac.cn

†These authors have contributed equally to this work

RECEIVED 22 February 2023
ACCEPTED 21 June 2023
PUBLISHED 30 June 2023

CITATION
Zhou X, Wang J, Li Q, Bai B, Mao F, Li X and Wang Y-Q (2023), Late Paleocene to early Oligocene fire ecology of the south Mongolian highland.
Front. Earth Sci. 11:1171452.
doi: 10.3389/feart.2023.1171452

Late Paleocene to early Oligocene fire ecology of the south Mongolian highland

Xinying Zhou[1,2†], Jian Wang[1,3†], Qian Li[1], Bin Bai[1], Fangyuan Mao[1], Xiaoqiang Li[1,2*] and Yuan-Qing Wang[1,2*]

[1]Key Laboratory of Vertebrate Evolution and Human Origins of Chinese Academy of Sciences, Institute of Vertebrate Paleontology and Paleoanthropology, Beijing, China, [2]College of Earth and Planetary Sciences, University of Chinese Academy of Sciences, Beijing, China, [3]Department of Archaeology and Anthropology, University of Chinese Academy of Sciences, Beijing, China

Changes in fire ecology during warm and cold periods in the geological past are important because of their effects on terrestrial ecosystems and the global carbon cycle. We examined the charcoal concentrations of the Erden Obo section in Inner Mongolia to reconstruct the evolution of wildfire and their relationship to the regional vegetation from the Late Paleocene through Early Oligocene. Our data show that fire frequency were relatively high from the end of the Paleocene to the beginning of the Eocene, in accord with other paleofire records worldwide. However, low fire frequency occurred during the Early Eocene Climate Optimum (EECO), coincident with the change in the regional vegetation from shrubland to forest due to the strengthening of the regional rainfall, and we suggest that the humid climate may have been responsible for this decrease. High frequency fire occurred after the Middle Eocene, near-synchronously with the transition of the regional vegetation from forest to steppe. The high-frequency fire was most likely triggered by regional drought during the aridification process after the Middle Eocene. We propose that these temporal changes in the fire ecology were consistent within the northern temperate zone from the Late Paleocene through Early Oligocene, and we suggest that studies of global wildfires need to be evaluated within the context of paleovegetation zones and ecosystem evolution.

KEYWORDS

fire ecology, Eocene, Mongolia highland, vegetation, Erden Obo, Erlian basin

1 Introduction

During the Eocene, ~56–33.9 million years ago (Ma), the global climate system experienced a series of major adjustments, including the Paleocene–Eocene Thermal Maximum (PETM), the Early Eocene Climate Optimum (EECO), the Middle Eocene Climate Optimum (MECO), and the Eocene-Oligocene transition (EOT) events, which comprised the warmest intervals within the entire Cenozoic (Zachos et al., 2001; Barnet et al., 2019). Studies of the changes in terrestrial ecosystems, the global carbon cycle, and the global climate during the warming and cooling events of the Eocene have contributed to an improved understanding of the interactions among the climate system and the carbon cycle on a global scale (McInerney and Wing, 2011; Sun et al., 2014; Barnet et al., 2019).

Fire is a key mechanism for facilitating rapid exchanges among terrestrial carbon pools and the atmospheric and oceanic carbon pools (Bond and Keeley, 2005; Lasslop et al., 2019), and it has long been an important component of Earth's terrestrial

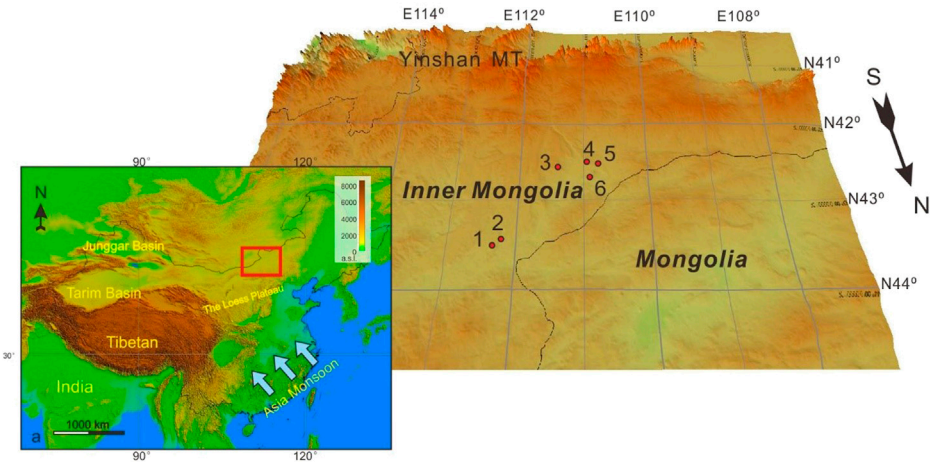

FIGURE 1
The study area, sedimentary section, and other sites mentioned in this study. 1. Arshanto; 2. Irdin Manha; 3. Erden Obo (this study); 4. Ulan Gochu; 5. Ula Usu; 6. Wulanhuxiu (modified from Wang et al., 2012; Bai et al., 2018).

ecosystems, affecting vegetation distributions, carbon cycling, and the global climate (Bond and Keeley, 2005; Reichstein et al., 2013; Lasslop et al., 2019). The ecological history of fire can provide important clues for understanding anomalous climate events from the Paleocene through Oligocene (Higgins and Schrag, 2004; Fung et al., 2019). The "wildfire hypothesis" proposed by Kurtz et al. (2003) suggests that widespread fire and peatland burning occurred globally at the Paleocene-Eocene transition, resulting in the release of huge quantities of light carbon during a brief interval (~0.17 Ma) and causing prominent negative $\delta^{13}C$ peak within benthic foraminifera in the global deep ocean. That ultimately triggered the Paleocene–Eocene Thermal Maximum (PETM) (Kurtz et al., 2003; Finkelstein et al., 2006). Although the "wildfire hypothesis" has been recently questioned, the role of terrestrial ecosystem changes and fire in explaining ocean carbon isotope records and global climate anomalies during the Paleocene remains important (McInerney and Wing, 2011; Fung et al., 2019). The key question is whether the terrestrial carbon pool could have released such a large amount of carbon in such a short interval, and we still lack extensive geological evidence to assess the extent and magnitude of the paleofires (Moore and Kurtz, 2008; McInerney and Wing, 2011).

The Mongolian Plateau is located on the edge of the current Asian summer monsoon system, and it is a key area for studying mammalian evolution and radiation (Meng et al., 1994; Wang et al., 2010). The Paleogene biostratigraphy of this region, based on fossil mammals, is by far the best documented within Asia (Bai et al., 2018; Li et al., 2018). Here, we present charcoal records from the Erden Obo section of the Erlian Basin in Inner Mongolia, which we use to reconstruct regional fire history and explore the fire dynamics from the Late Paleocene through Early Oligocene. Our results contribute to an improved understanding of the linkages among climate, vegetation and fire, with implications for predicting the rate and magnitude of future global warming.

2 Regional setting and research materials

The Erlian Basin, which today is part of the central and northern parts of Inner Mongolia Autonomous Region, is located on the edge of the East Asian monsoon and on the boundary between the North China and Siberian Plate. The basin is one of the large onshore sedimentary basins of East Asia and is ~1,000 km long from east to west and 20–220 km wide from north to south, with the total area of 101,000 km^2, bounded by the Songliao Basin to the east, the Hailar-Tamsag Basin and the East Gobi Basin to the north, and the Yingen-Ejinaqi Basin to the west (Meng et al., 2003). Meteorological records indicate modern annual precipitation is 139 mm, with the annual mean temperature varying between −2°C and 11°C, and 4.5°C on average. Recorded summer high temperatures can reach 41°C and winter temperatures are as low as −40°C.

The Erden Obo section in the central Erlian Basin is one of the most important Paleogene mammal fossil sites in the Mongolian highland (Figure 1). The Erden Obo [reported in Osborn (1929) as Urtyn Obo] section was first reported by Osborn (1929), based on Granger's (1928) sketch. Osborn (1929) divided the section into eight units from bottom to top (Figure 2): "Basal Red," "Basal White," "Lower Red," "Lower White" (19.8 m), "Middle Red" (21.3 m), "Middle White or Gray" (9.1 m), "Upper Red" (29.0 m), and "Upper White" (7.6 m) (Granger, 1928). The "red layer" is composed mainly of brick-red mudstone with muddy siltstone and silty mudstone, while the "white layer" consists mainly of fine or medium sand, coarse sandstone, and conglomerates. The sedimentary environment of these strata is flood plain, shallow lake and river sediment interbed.

In this study, we collected sediment samples from the Erden Obo section, following Granger's (1928) simple stratigraphic division; however, we remeasured the section with a level and the base was extended downwards. Our new measurements show that the thickness of the Erden Obo section from top to bottom is ~189 m, including 0–11.7 m for the upper white, 11.7–50.2 m for

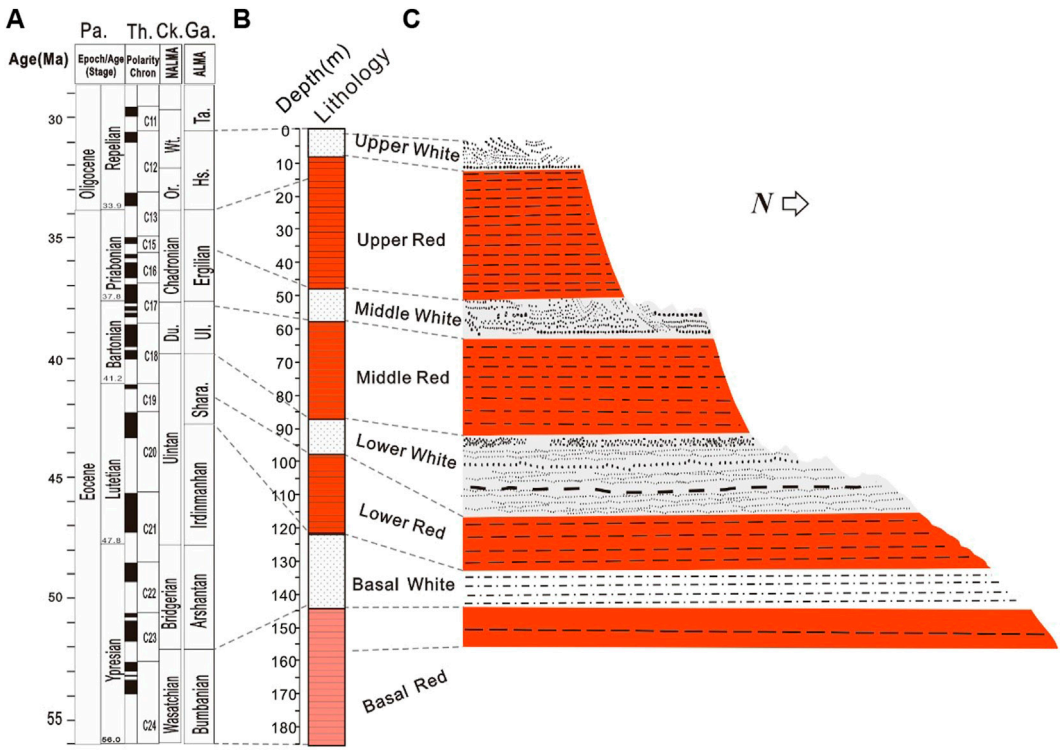

FIGURE 2
Biochronology based on large mammal fossils of the Erden Obo section (according to Bai et al., 2018). **(A)** Standard paleomagnetic stratigraphy, North American land mammal ages (NALMA), and Asian land mammal ages (ALMA). **(B)** Lithology of the Erden Obo section. **(C)** Field sketch of the Erden Obo section (Granger, 1928).

the upper red, 50.2–58.5 m for the middle white layer, 58.5–89.2 m for the middle red layer, 89.2–99.4 m for the lower white, 99.4–122.7 m for the lower red, 122.7–146 m for the bottom white, and 146–189 m for the basal red. Samples were collected from the bottom of the section downward at an average interval of 1.2 m. Around 1 kg of sediment was collected for each sample and the samples were taken from all eight deposition units.

3 Stratigraphy and chronology

The stratigraphic range of the Erlian Basin is nearly continuous from the Late Paleocene through Early Oligocene, and almost all the Eocene ALMAs except Bumbanian and Ergilian are based on the corresponding faunas of the basin. Various large and small mammalian fossils have been reported from different units at Erden Obo and they have contributed to the refinement of biostratigraphic correlations with other localities in the Erlian Basin (Jiang, 1983; Qi, 1990). The age determination of the Erden Obo section in this study is based mainly on biostratigraphic correlations (Figure 2A).

In the biostratigraphic correlations made in the 1930s, the "Basal Red" was regarded as the same stage as the Arshanto Formation, suggesting that the basal age was ~50 Ma (Osborn, 1929). Wang et al. (2012) suggested that the "Basal Red" should be the Nomogen Formation and the "Upper White" should be the upper Naogangdai Formation, while the correlation of the other layers at Erden Obo remains unclear (Wang et al., 2012). The magnetostratigraphic results for the Nohe Timbur and Huhe Boerhe sections show that the Nomogen Formation was mainly deposited from the Late Paleocene through earliest Eocene, with the age range of ~59.2–54.8 Ma. The Ashantou Formation spans the Early and Middle Eocene, with the age range of ~54.1–48.2 Ma. The age of the Ildinmanha Formation is Middle Eocene, constrained to ~48–47 Ma (Sun et al., 2009). Bai et al. (2018) comprehensively analyzed the temporal and spatial distribution of Paleogene perissodactyl species in the Erlian Basin based on published specimens and accordingly revised the most complete sedimentary section at Erden Obo, with the age range from Late Paleocene through Early Oligocene (Figures 2B, C).

Previous studies of the biostratigraphy and magnetostratigraphy (unpublished data) indicate that the depositional history of the Erden Obo section commenced at the end of the Paleocene and spans the early middle and late Eocene through Early Oligocene with the approximate age range of 55–30 Ma. Considering multiple factors, the chronostratigraphic framework referenced in this study is the same as that established by Bai et al. (2018) and Li et al. (2018).

4 Charcoal analysis

Charcoal is a direct product of the incomplete combustion of plant bodies by fire, and the concentration and frequency of charcoal

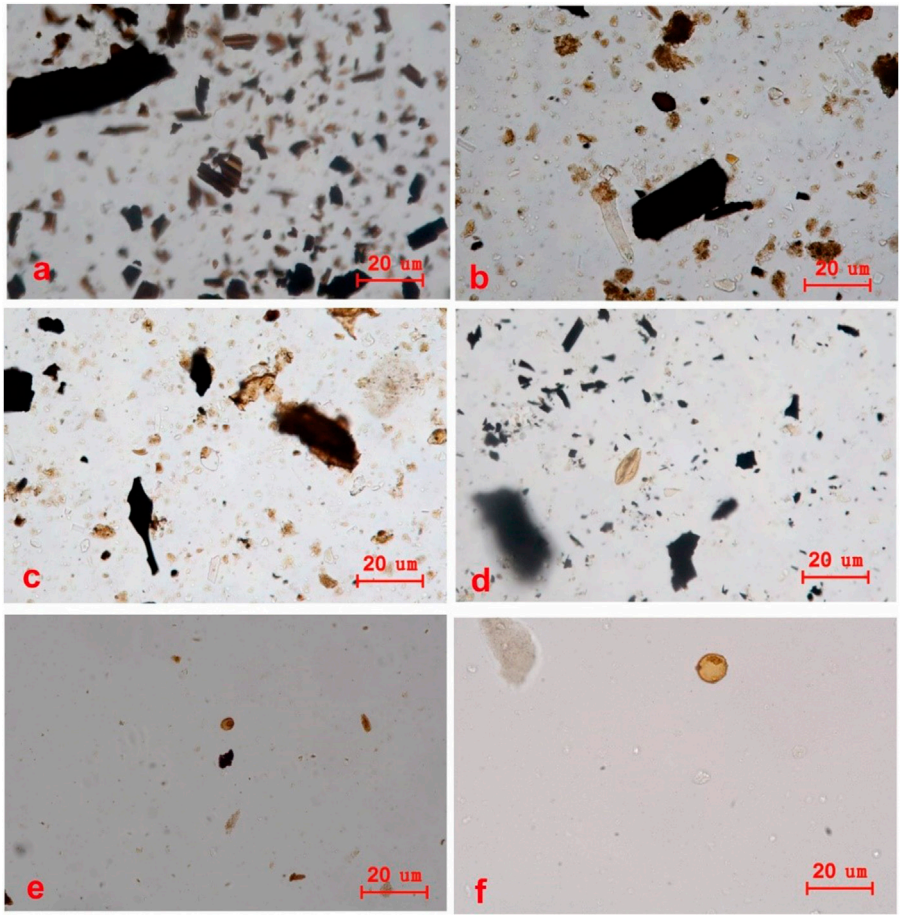

FIGURE 3
Microscope photographs of various concentrations of charcoal particles in pollen slides from the Erden Obo section. **(A,B)** High concentration sample (No. NN065, 99.4 m). **(C,D)** Moderate concentration sample (No. NN154, 10.2 m). **(E,F)** Low concentration sample (No. NN036, 146.7 m).

in the sediment indicate the intensity and frequency of paleo fire (Higuera et al., 2007). Fire history reconstruction inferred from sedimentary charcoal records is based on measuring screened charcoal area, estimating fragment volume, or counting fragment (Leys, B., et al., 2013). The reconstruction based on charcoal area is more explicit and stable than the reconstruction based on debris count (Leys, B., et al., 2013). Area-based reconstruction rather than particle counting methods should be used when debris is likely to affect debris abundance (Leys, B., et al., 2013; Higuera et al., 2007.

The microscopic charcoal particles encountered on pollen slides in this study were quantified with the point count method (Clark, 1982). Differences in charcoal size and size-class distribution are mainly caused by different preparation techniques (Tinner and Hu, 2003). This method provides a probability-based estimate of the Charcoal Area Concentration (CAC) of sediment samples, enabling the rapid quantification of the area rather than the total number of charcoal particles on a pollen slide, and the area and number concentrations of charcoal particles are highly correlated in standard pollen slides (Tinner and Hu, 2003). Hence it is not biased by the fragmentation of charcoal particles that occurs during pollen extraction or by sediment diagenesis (Clark, 1982). A total of 83 samples were collected between 0–190 m for microcharcoal analysis. For each sample, ~150 g of sediment was processed using standard palynological preparation procedures. The extraction procedures are as follows: sample was used for pollen analysis and pretreatment consisted of the following stages: 1) Addition of hydrochloric acid to remove carbonates; 2) flotation with 2.0 second-class heavy liquid flotation (with ZnCl2 and KI-ZnI2); 3) addition of a 1:9 solution of concentrated sulfuric acid and acetic anhydride; 4) suspension in glycerol and mounting on microscope slides.

One tablet containing a known number of *Lycopodium* spores (27,560) was added to estimate microcharcoal concentrations. Microscopic charcoal was point-counted during palynological identification, and each sample was examined at ×400 magnification for 500 fields of view (FOV) on pollen slides. The charcoal area concentration was calculated as:

$$Y = \frac{C}{M} \times \frac{L}{l} \times \frac{S}{G} \ (cm^2/g)$$

where Y is the charcoal area concentration (cm^2/g), C is the number of points covered by the counted charcoal, M is the total number of points in the 500 FOVs (5500 in this study), L is the number of *Lycopodium* spores (=27,560), l is the number of *Lycopodium* spores

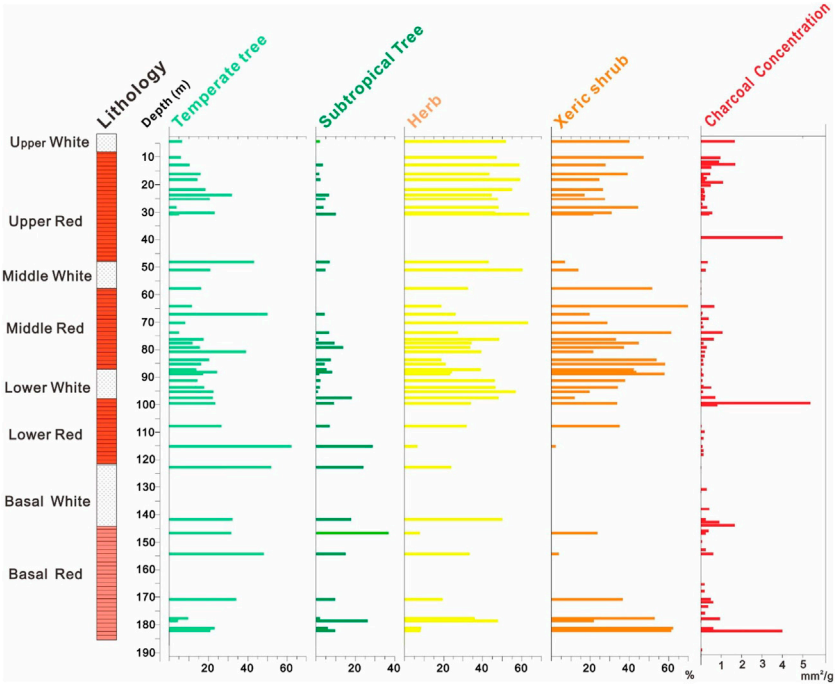

FIGURE 4
Depth profiles of microcharcoal concentrations and the percentages of selected pollen taxa within the Erden Obo section.

counted, S is the area of 500 FOVs (≈4.54 × 10^2 mm^2), and G is the weight of each sample (150 g).

5 Results

Examples of different microcharcoal concentrations in the sediments of Erden Obo are shown in Figure 3. The microcharcoal concentrations and pollen data were used to assess the dynamics of the regional vegetation and fire activity (Li et al., 2005; Miao et al., 2022). Charcoal particles were observed in 78 out of 83 samples, but the CAC values were low on average and they fluctuated substantially. The overall mean CAC is 0.493 mm^2/g and 39 samples had values <0.2 mm^2/g. Only 23 samples were above the mean value of 0.493 mm^2/g, and 8 samples had values >1 mm^2/g. Peak values were 4.008 mm^2/g at 182.2 m, 4.015 mm^2/g at 39.2 m, and 5.382 mm^2/g at 99.4 m, which is around ten times the overall mean value.

Overall, the CAC records show a high-low-high temporal pattern. First peak value of 4.01 mm^2/g occurs at the base of the profile (182.2 m), and the mean value (174–180 m) is also relatively high. In contrast, the mean value (0.326 mm^2/g) in the middle and lower middle parts of the section (105–174 m) is lower overall, and no charcoal particles were observed in the samples from the depths of 107.7, 122.7, and 131.7 m. However, the CAC increases abruptly above 100 m and reaches the maximum value (5.38 mm^2/g), while the CAC increases significantly above 40 m and reaches a third peak.

The charcoal area concentrations correlate quite well with the pollen stratigraphy (Figure 4). From the pollen data, the tree taxa occupied a large proportion in the early Eocene, but decreased significantly after about 42 Ma. At the same time, the types of herbaceous and xerophytic shrub increased dramatically. And there were several notable fluctuations. Stratigraphic levels with high charcoal concentrations are generally associated with lower tree pollen concentrations, especially subtropical taxa, and the microcharcoal concentrations are better correlated with higher proportions of xerophytic shrubs and herbaceous taxa. Additionally, considering that both high and low microcharcoal concentrations occur in both the white sandstone and red mudstone layers, there appears to be no relationship between the sedimentary facies and microcharcoal concentrations.

6 Discussion

Based on mammal fossils unearthed in Erden Obo section, the fauna of North America and the regional Palaeogene biostratigraphy, the age of Erden Aobao section has been determined to be from late Paleocene to Early Oligocene, including the early, middle and late Eocene strata, spanning about 56–30 Ma (Bai et al., 2018; Li et al., 2018). The stratigraphic-chronological correlation lines in Figures 2, 5 are shown, it is more certain that the “Basal Red” and Bumbanian Formation are at the same time, the date is late Paleocene-early Eocene, roughly 56–52 Ma; “Basal White” corresponds to Arshantan Formation (Early Eocene) and Irdinmanhan Formation (Middle Eocene), roughly 52–43 Ma; “Lower Red” corresponds to the lower part of Sharamulun Formation (Shara.) roughly 43–41 Ma; “Lower White” is equivalent to the upper of Sharamulun Formation, roughly 41–40 Ma; “Middle red” corresponds to Ulangechu (Ul.),

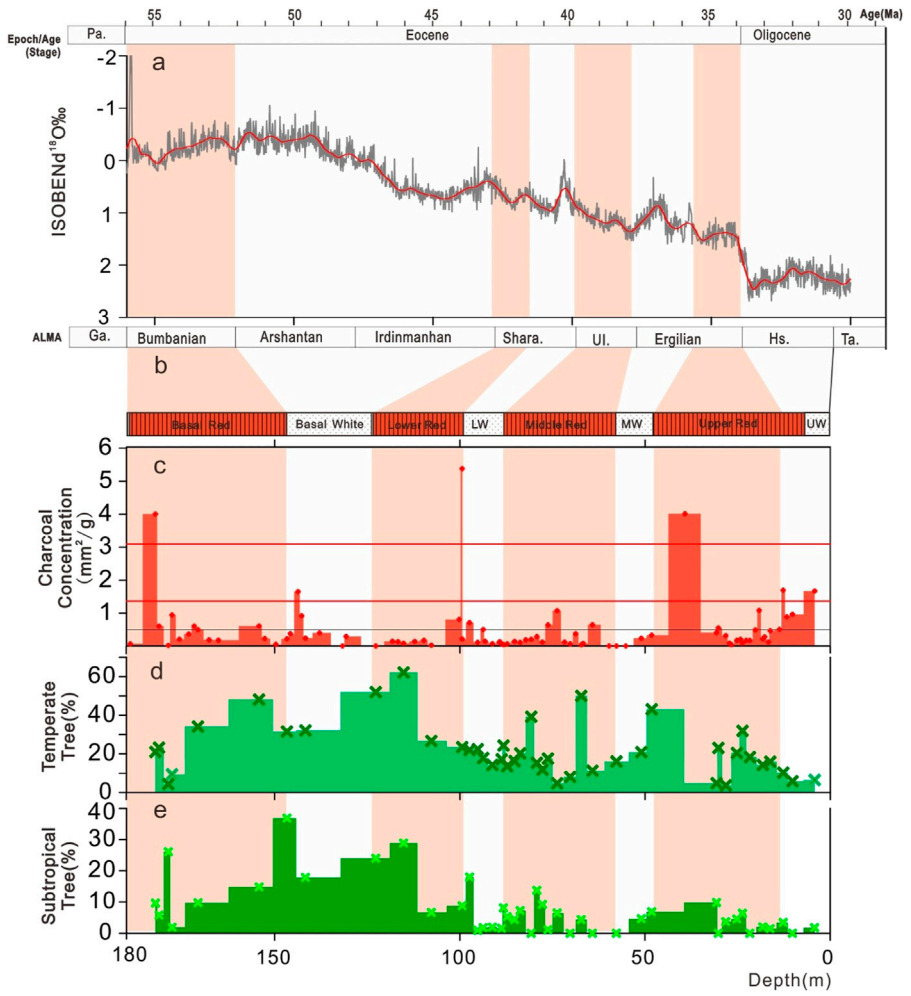

FIGURE 5
Comparison of fire evolution mechanisms and global changes on the Mongolian Plateau. **(A)** Global temperature as indicated by the benthic foraminiferal $\delta^{18}O$ record (Westerhold et al., 2020). **(B)** Correlation of the ALMA and the mammalian chronostratigraphy of the Erden Obo section. **(C)** CAC of the Erden Obo section. **(D,E)** Percentages of temperate and subtropical trees of the Erden Obo section. The pink shading represents geological ages corresponding to the lithostratigraphy of the Erden Obo section, based on the comparison of the ALMA.

roughly 40–38 Ma; "Middle White" is equivalent to the lower of the Erglian formation, roughly 38–36 Ma; The lower part of "Upper Red" corresponds to the upper part of the Erglian formation, roughly 36–34 Ma; The upper part of "Upper Red" and "Upper White" belong to the Oligocene, about 34–30 Ma.

Although the age of the Erden Obo section spans 56–30 Ma, the PETM event (~55.8 Ma) may not have been resolved using our data as it lasted only 0.17 Myr (Röhl et al., 2007), and the CAC data from Erden Obo are of insufficient resolution (~0.25 Myr) to capture it. Additionally, although the Erden Aobao section includes the most complete strata in Erlian Basin from the end of Paleocene to the early Oligocene, a regional sedimentary discontinuity and stratigraphic deficiencies may exist in the area. Nevertheless, the CAC data provide an overview of the Paleogene fire history on the south Mongolian Plateau, including the EECO, MECO, and EOT.

Our CAC record suggests that fires were infrequent in Erlian basin during the Late Paleocene through Early Oligocene, at least compared with Quaternary fire records from the surrounding area. Nearby Quarternary loess sediments had an average CAC of ~1–3 mm^2/g in Quaternary loess sediments adjacent to our study area (Li et al., 2009), and a CAC range of 0.03–57.77 mm^2/g in the Holocene sediments of Northeast China, with the average of 7.12 mm^2/g (Li et al., 2005). CAC values were as high as 100 mm^2/g during the late Holocene, as the result of anthropogenic factors (Li et al., 2007). In contrast, the mean CAC at Erden Obo is only 0.493 mm^2/g, with around half of the data values <0.2 mm^2/g. This indicates that fire activity on the Mongolian Plateau from the end of the Paleocene to the beginning of the Oligocene, including the entire Eocene, was relatively low compared to the Quaternary in northern China.

The modern global distribution of natural fires shows that high-frequency fires occur mainly in areas with strong seasonality, such as in seasonal rainforest in typical monsoon zones (Southeast Asia, South China) and shrub-steppe (Eastern Europe, eastern Inner Mongolia steppe) (Bond and Keeley, 2005; Reichstein et al., 2013; Hantson et al., 2015). Enhanced interannual climate variability,

i.e., extremely wet years followed by exceptionally dry years, promotes favorable fire conditions because of the annual accumulation of sufficient amounts of fuel-producing vegetation (e.g., grass) (Margolis and Balmat, 2009). Prolonged dry periods lead to widespread fires, which spread rapidly during the long dry season. In addition, fires may be less frequent during prolonged droughts if there is insufficient combustible biomass, while the vegetation composition and fire-prone plant taxa are also important factors in determining the fire propensity (Flannigan et al., 2009).

The temporal variations of our paleofire data may be related to the seasonal precipitation distribution and vegetation characteristics (Figure 5). High-latitude Sea surface temperatures (SST) increased by 10°C due to the high global temperatures in the Eocene (Zachos et al., 2001; Pearson et al., 2009). Tree taxa in tropical and subtropical areas, such as *Cycads*, *Pinus*, *Podocarpus*, *Rhus*, and Moraceae were widely distributed in the modern temperate regions of the Northern Hemisphere, suggesting a lower winter-summer temperature difference in northern temperate regions at that time (McInerney and Wing, 2011; Eberle and Greenwood, 2012; Lauretano et al., 2015). On the other hand, in terms of precipitation, the modern monsoon had not formed because the Tibetan Plateau did not yet exist, and water vapor from the Indian Ocean could not penetrate deeply into the Asian interior (Zhang et al., 2012). However, this effect during the EECO appears to have been offset by the increased precipitation in this region due to water vapor exchanges over land and sea driven by high temperatures (Quan et al., 2012; Licht et al., 2014). The precipitation in this region includes two components: sourced from the western Pacific and Indian Ocean in summer, and from the westerly belt in winter (Li et al., 2023). Therefore, the difference between dry and wet conditions in winter and summer was not significant, and as a result, the fire frequency throughout the Eocene was less frequent and intense than in modern monsoon rainforest and shrubland.

In terms of evolutionary trends, a significant three-stage (strong-weak-strong) temporal pattern is evident in Figures 4, 5. The microcharcoal concentration was the lowest in the Early Eocene (53–42 Ma, depth range 146–105 m), and no microcharcoal was visible in many layers. By contrast, CAC was much higher in the basal and upper parts of sections, indicating relatively intense fire activity during the Paleocene–Eocene transition and Early Eocene (depth interval 189–146 m, ~55–53 Ma) and the Late Eocene–Early Oligocene (depth interval 40–0 m, ~36–32 Ma). The degree of variation in charcoal concentrations of Erden Obo section is typical in studies of paleofire activity. Previous studies have shown that large wildfires typically burn hundreds of times as much woodland as ordinary fires (Artés et a., 2019), and that orders of magnitude differences in the amount of charcoal deposited on the ground can sometimes even be observed with the naked eye in the field.

Despite the relatively limited global data on Paleocene fires, it appears that the Late Paleocene–Early Eocene transition had a higher fire frequency than the EECO. Charcoal and palynological data from the Cobham lignite bed in southern England suggest that fire was sporadic in the Late Paleocene (Collinson et al., 2009), and that Eocene vegetation was characterized by a decrease in ferns, an increase in wetland plants, and a decrease in fire occurrence. Robson et al. (2015) studied 11 lignite seams within the Schöningen coal deposits in Germany and concluded that charcoal percentages during the Early Eocene did not indicate an increase in fire activity during the EECO.

Additionally, the record of particulate organic matter from IODP Site 302 suggests that fire activity was more active in the Paleocene than in the Early Eocene on land around the Arctic Ocean (Denis et al., 2017). These findings imply that the frequency and intensity of fire decreased from the Paleocene to the EECO, at least in the northern temperate zone (modern) during the Eocene, even though the EECO was the warmest period of the entire Cenozoic. High temperatures and seasonal drought have traditionally been considered to trigger fires (Flannigan et al., 2009). However, high heat exchange at the Earth's surface facilitated water exchange between the atmosphere, ocean, and land during the Early Eocene (Bowen et al., 2004; Licht et al., 2014), which resulted in the Earth acting more like a "steamer" than a "pan" (i.e., hot and humid rather than hot and dry) during the EECO. In short, the warm and humid global environment at this time led to a decrease in regional fire.

The proportion of temperate and subtropical trees in Erden Obo section was the highest during the EECO, indicating a relatively closed wet and warm forest ecosystem, which is in sharp contrast to the present-day desert-steppe with annual rainfall <150 mm (Wang et al., 2022). The increase in forest during the EECO occurred not only on the Mongolian Plateau but also on a global scale (Greenwood and Wing, 1995; Bowen et al., 2004; Eberle and Greenwood, 2012). At the same time, the Green River Formation of Utah and Colorado in North America was deposited within a set of large, unusually productive lakes (West et al., 2020), and subtropical palms and ginkgo trees expanded to Antarctica during the EECO. These observations reflect the fact that, at least during the EECO, global extreme heat caused warm and humid atmospheric circulation that promote the global expansion of tropic and subtropical forest, including inland Asia. After that, with the decrease of global temperature aroude 43 Ma, the proportion of trees in Erden Aobao section also decreased significantly. We can see the correlation between climate—vegetation and fire in our study area from the correlation between charcoal and pollen data.

The CAC data from the Erden Obo section recorded at least three major fire intervals during the Eocene. These events may be related to seasonal drought caused by abrupt global climate cooling during the Eocene, as the pollen evidence shows that these intervals are correlative with a decrease in tree pollen and an increase in herbaceous and xerophytic shrub pollen. Overall, regional fire activity was closely related to the evolution of the regional vegetation ecosystem. For example, several researchers have proposed that angiosperms triggered a new fire regime in the Cretaceous, which promoted the spread of angiosperms (Bond and Scott, 2010).

The fire intensity in the study region began to increase after around the Middle Eocene (depth 100 m, ~42 Ma), while the proportion of trees began to decrease and herbs and xerophytes increased significantly. Subsequently, during the Late Eocene (depth 45 m, ~37 Ma), the frequency and intensity of fires increased, accompanied by the maximum proportion of herbaceous vegetation. This process suggests that global temperatures decreased in the Middle and Late Eocene to Oligocene, and the

increased seasonal drought in temperate regions led to increased fire activity (Liu et al., 2009; Abels et al., 2011; Sun et al., 2014). We suggest that this dynamic change contributed to the evolution of steppe ecosystems and eventually to the formation of the northern steppe during the Oligocene.

In general, our CAC data from the Erden Aobao section indicate that wildfire activity in the Mongolian Plateau is associated with global temperature changes in a negative feedback mechanism from the end of the Paleocene to the beginning of the Oligocene, which is consistent with previous records in Europe and North America. The terrestrial vegetation system was closely related to fire activity. During the early Eocene warm period, the region's sub-tropical and temperate mixed woodland developed, and the regional climate became humid and the frequency of fire decreased. However, when the global temperature decreased in the middle and late Eocene, the regional grasslands/shrubs expanded, and fire activity began to increase. This means that when global temperatures are lower, more light carbon is released from terrestrial carbon pools through fire activity and deposited into oceans and lakes.

7 Conclusion

The CAC and palynological data for the Erden Obo section provide a history of the evolution of the fire ecology on the south Mongolian Plateau from the Late Paleocene through Early Oligocene. The overall low mean CAC values indicate that the Eocene fire activity on the Mongolian Plateau was less frequent and intense than within modern monsoon rainforest and shrubland. Fire activity was stronger during the Paleocene–Eocene and Late Eocene–Early Oligocene transition (depth interval 40–0 m) than during the EECO. Global high-temperature systems led to a wetter northern temperate zone during the EECO and regional fire activity was suppressed. Global temperatures decreased during the Middle and Late Eocene–Oligocene, increasing the occurrence of seasonal drought in temperate regions and leading to increased fire activity. All these factors together contributed to the evolution of the northern temperate grassland ecosystem in the Oligocene.

Data availability statement

The raw data supporting the conclusion of this article will be made available by the authors, without undue reservation.

Author contributions

Y-QW, XL and XZ designed the study. All authors participated in the fieldwork. FM performed the sample collection. JW and XZ conducted the experiments and data analysis. XZ and JW wrote the first draft. XL, Y-QW, BB and QL reviewed the final manuscript. All authors contributed to the paper and approved the submitted version.

Funding

This work is supported by the National Key Research and Development Program of China (22022YFF0801102), the CAS Project for Young Scientists in Basic Research (YSBR-019), the Strategic Priority Research Program of Chinese Academy of Sciences (XDB26000000), the National Natural Science Foundation of China (NSFC 41888101), and the Youth Innovation Promotion Association of the Chinese Academy of Sciences (2022071).

Acknowledgments

We would like to thank Dr. Yanxin Gong and Rancheng Xu for discussions on biostratigraphic comparisons in the Erlian Basin. Sincere thanks to Junnan Xu, Huihai Wang and Zhongshen Wang for pollen experiments. We are grateful to Prof. Jan Bloemendal for considerably improving the English language. The authors gratefully acknowledge the Handling Editor OV and two reviewers for their professional review comments.

Conflict of interest

The authors declare that the research was conducted in the absence of any commercial or financial relationships that could be construed as a potential conflict of interest.

Publisher's note

References

Abels, H. A., Dupont-Nivet, G., Xiao, G., Bosboom, R., and Krijgsman, W. (2011). Step-wise change of asian interior climate preceding the eocene–oligocene transition (EOT). *Palaeogeogr. Palaeoclimatol. Palaeoecol.* 299, 399–412. doi:10.1016/j.palaeo.2010.11.028

Artés, T., Oom, D., de RigoDurrant, D. T., Maianti, P., Libertà, G., San-Miguel-Ayanz, J., et al. (2019). A global wildfire dataset for the analysis of fire regimes and fire behaviour. *Sci. Data* 6, 296. doi:10.1038/s41597-019-0312-2

Bai, B., Wang, Y.-Q., Li, Q., Wang, H.-B., Mao, F.-Y., Gong, Y.-X., et al. (2018). Biostratigraphy and diversity of Paleogene perissodactyls from the Erlian Basin of inner Mongolia, China. *Am. Mus. Novitates* 3914, 1–60. doi:10.1206/3914.1

Barnet, J. S. K., Littler, K., Westerhold, T., Kroon, D., Leng, M. J., Bailey, I., et al. (2019). A high-fidelity benthic stable isotope record of late cretaceous–early Eocene climate change and carbon-cycling. *Paleoceanogr. Paleoclimatology* 34, 672–691. doi:10.1029/2019pa003556

Bond, W. J., and Keeley, J. E. (2005). Fire as a global 'herbivore': The ecology and evolution of flammable ecosystems. *Trends Ecol. Evol.* 20, 387–394. doi:10.1016/j.tree.2005.04.025

Bond, W. J., and Scott, A. C. (2010). Fire and the spread of flowering plants in the Cretaceous. *New Phytol.* 188, 1137–1150. doi:10.1111/j.1469-8137.2010.03418.x

Bowen, G. J., Beerling, D. J., Koch, P. L., Zachos, J. C., and Quattlebaum, T. (2004). A humid climate state during the Palaeocene/Eocene thermal maximum. *Nature* 432, 495–499. doi:10.1038/nature03115

Clark, R. L. (1982). Point count estimation of charcoal in pollen preparations and thin sections of sediments. *Pollen Spores* 24, 523–535.

Collinson, M. E., Steart, D. C., Harrington, G. J., Hooker, J. J., Scott, A. C., Allen, L. O., et al. (2009). Palynological evidence of vegetation dynamics in response to palaeoenvironmental change across the onset of the paleocene-eocene thermal maximum at Cobham, southern England. *Grana* 48, 38–66. doi:10.1080/00173130802707980

Denis, E. H., Pedentchouk, N., Schouten, S., Pagani, M., and Freeman, K. H. (2017). Fire and ecosystem change in the arctic across the paleocene–eocene thermal maximum. *Earth Planet. Sci. Lett.* 467, 149–156. doi:10.1016/j.epsl.2017.03.021

Eberle, J. J., and Greenwood, D. R. (2012). Life at the top of the greenhouse Eocene world—a review of the Eocene flora and vertebrate fauna from Canada's high arctic. *GSA Bull.* 124, 3–23. doi:10.1130/b30571.1

Finkelstein, D. B., Pratt, L. M., and Brassell, S. C. (2006). Can biomass burning produce a globally significant carbon-isotope excursion in the sedimentary record? *Earth Planet. Sci. Lett.* 250, 501–510. doi:10.1016/j.epsl.2006.08.010

Flannigan, M. D., Krawchuk, M. A., De Groot, W. J., Wotton, B. M., and Gowman, L. M. (2009). Implications of changing climate for global wildland fire. *Int. J. wildland fire* 18, 483–507. doi:10.1071/wf08187

Fung, M., Schaller, M., Hoff, C., Katz, M., and Wright, J. (2019). Widespread and intense wildfires at the Paleocene-Eocene boundary. *Geochem. Perspect. Lett.* 10, 1–6. doi:10.7185/geochemlet.1906

Granger, W. (1928). "Records of fossils collected in Mongolia. Central asiatic expeditions," in *Field books of the third asiatic expedition RBC51-E* (New York, NY, United States: American Museum of Natural History Library), 1–77.

Greenwood, D. R., and Wing, S. L. (1995). Eocene continental climates and latitudinal temperature gradients. *Geology* 23, 1044–1048. doi:10.1130/0091-7613(1995)023<1044:eccalt>2.3.co;2

Hantson, S., Pueyo, S., and Chuvieco, E. (2015). Global fire size distribution is driven by human impact and climate. *Glob. Ecol. Biogeogr.* 24, 77–86. doi:10.1111/geb.12246

Higgins, J. A., and Schrag, D. P. (2004). *Model simulations of the global carbon and sulfur cycles: Implications for the paleocene-eocene thermal maximum*. Washington, D.C., United States: American Geophysical Union.

Higuera, P. E., Peters, M. E., Brubaker, L. B., and Gavin, D. G. (2007). Understanding the origin and analysis of sediment-charcoal records with a simulation model. *Quat. Sci. Rev.* 26, 1790–1809. doi:10.1016/j.quascirev.2007.03.010

Jiang, H. X. (1983). Division of the Paleogene in the Erlian Basin of inner Mongolia. *Geol. Inn. Mogolia* 55, 18–36.

Kurtz, A. C., Kump, L. R., Arthur, M. A., Zachos, J. C., and Paytan, A. (2003). Early Cenozoic decoupling of the global carbon and sulfur cycles. *Paleoceanography* 18. doi:10.1029/2003pa000908

Lasslop, G., Coppola, A. I., Voulgarakis, A., Yue, C., and Veraverbeke, S. (2019). Influence of fire on the carbon cycle and climate. *Curr. Clim. Change Rep.* 5, 112–123. doi:10.1007/s40641-019-00128-9

Lauretano, V., Littler, K., Polling, M., Zachos, J. C., and Lourens, L. J. (2015). Frequency, magnitude and character of hyperthermal events at the onset of the Early Eocene Climatic Optimum. *Clim. Past* 11, 1313–1324. doi:10.5194/cp-11-1313-2015

Leys, B., Carcaillet, C., Dezileau, L., Ali, A. A., and Bradshaw, R. H. W. (2013). A comparison of charcoal measurements for reconstruction of Mediterranean paleo-fire frequency in the mountains of Corsica. *Quat. Res.* 79, 337–349. doi:10.1016/j.yqres.2013.01.003

Li, H., Yang, X., Scuderi, L. A., Hu, F., Liang, P., Jiang, Q., et al. (2023). East Gobi megalake systems reveal East Asian Monsoon dynamics over the last interglacial-glacial cycle. *Nat. Commun.* 14, 2103. doi:10.1038/s41467-023-37859-1

Li, Q., Mao, F.-Y., and Wang, Y.-Q. (2018). First record of Eocene fossil rodent assemblages from the lower part of the erden Obo section, Erlian Basin (nei mongol, China) and its biochronological implications. *Palaeobiodiversity Palaeoenvironments* 98, 259–276. doi:10.1007/s12549-017-0303-2

Li, X., Shang, X., Dodson, J., and Zhou, X. (2009). Holocene agriculture in the Guanzhong Basin in NW China indicated by pollen and charcoal evidence. *Holocene* 19, 1213–1220. doi:10.1177/0959683609345083

Li, X., Zhao, H., Yan, M., and Wang, S. (2005). Fire variations and relationship among fire and vegetation and climate during Holocene at sanjiang Plain,Northeast China. *Sci. Geogr. Sin.* 25, 177–182. doi:10.13249/j.cnki.sgs,2005.02.177

Li, X., Zhou, X., Zhou, J., Dodson, J., Zhang, H., and Shang, X. (2007). The earliest archaeobiological evidence of the broadening agriculture in China recorded at Xishanping site in Gansu Province. *Sci. China Ser. D Earth Sci.* 50, 1707–1714. doi:10.1007/s11430-007-0066-0

Licht, A., Van Cappelle, M., Abels, H. A., Ladant, J. B., Trabucho-Alexandre, J., France-Lanord, C., et al. (2014). Asian monsoons in a late Eocene greenhouse world. *Nature* 513, 501–506. doi:10.1038/nature13704

Liu, Z., Pagani, M., Zinniker, D., Deconto, R., Huber, M., Brinkhuis, H., et al. (2009). Global cooling during the eocene-oligocene climate transition. *Science* 323, 1187–1190. doi:10.1126/science.1166368

Margolis, E. Q., and Balmat, J. (2009). Fire history and fire–climate relationships along a fire regime gradient in the Santa Fe Municipal Watershed, NM, USA. *For. Ecol. Manag.* 258, 2416–2430. doi:10.1016/j.foreco.2009.08.019

Mcinerney, F. A., and Wing, S. L. (2011). The paleocene-eocene thermal maximum: A perturbation of carbon cycle, climate, and biosphere with implications for the future. *Annu. Rev. Earth Planet. Sci.* 39, 489–516. doi:10.1146/annurev-earth-040610-133431

Meng, J., Wyss, A. R., Dawson, M. R., and Zhai, R. (1994). Primitive fossil rodent from Inner Mongolia and its implications for mammalian phylogeny. *Nature* 370, 134–136. doi:10.1038/370134a0

Meng, Q., Hu, J., Jin, J., Zhang, Y., and Xu, D. (2003). Tectonics of the late Mesozoic wide extensional basin system in the China-Mongolia border region: Wide extensional basin system. *Basin Res.* 15, 397–415. doi:10.1046/j.1365-2117.2003.00209.x

Miao, Y., Nie, J., Hu, X., Wan, Z., Zhao, B., Zhao, Y., et al. (2022). Wildfire history and savanna expansion across southern Africa since the late Miocene. *Palaeogeogr. Palaeoclimatol. Palaeoecol.* 603, 111189. doi:10.1016/j.palaeo.2022.111189

Moore, E. A., and Kurtz, A. C. (2008). Black carbon in paleocene–eocene boundary sediments: A test of biomass combustion as the PETM trigger. *Palaeogeogr. Palaeoclimatol. Palaeoecol.* 267, 147–152. doi:10.1016/j.palaeo.2008.06.010

Osborn, H. F. (1929). Embolotherium, gen. Nov., of the ulan gochu, Mongolia. *Am. Mus. Novitates* 353, 1–20.

Pearson, P. N., Foster, G. L., and Wade, B. S. (2009). Atmospheric carbon dioxide through the Eocene–Oligocene climate transition. *Nature* 461, 1110–1113. doi:10.1038/nature08447

Qi, T. (1990). A Paleogene section at erden Obo, nei mongol and on the discovery of pastoralodon lacustris (pantodonta, mammalia) in that area. *Vertebr. Palasiat.* 28, 25–33. doi:10.19615/j.cnki.1000-3118.1990.01.003

Quan, C., Liu, Y.-S., and Utescher, T. (2012). Eocene monsoon prevalence over China: A paleobotanical perspective. *Palaeogeogr. Palaeoclimatol. Palaeoecol.* 365-366, 302–311. doi:10.1016/j.palaeo.2012.09.035

Reichstein, M., Bahn, M., Ciais, P., Frank, D., Mahecha, M. D., Seneviratne, S. I., et al. (2013). Climate extremes and the carbon cycle. *Nature* 500, 287–295. doi:10.1038/nature12350

Robson, B. E., Collinson, M. E., Riegel, W., Wilde, V., Scott, A. C., and Pancost, R. D. (2015). Early Paleogene wildfires in peat-forming environments at Schöningen, Germany. *Palaeogeogr. Palaeoclimatol. Palaeoecol.* 437, 53–62. doi:10.1016/j.palaeo.2015.07.016

Röhl, U., Westerhold, T., Bralower, T. J., and Zachos, J. C. (2007). On the duration of the Paleocene-Eocene thermal maximum (PETM). *Geochem. Geophys. Geosystems* 8. doi:10.1029/2007gc001784

Sun, B., Yue, L. P., Wang, Y. Q., Meng, J., Wang, J. Q., and Xu, Y. (2009). Magnetostratigraphy of the early Paleogene in the Erlian Basin. *J. Stratigr.* 33, 62–68.

Sun, J., Ni, X., Bi, S., Wu, W., Ye, J., Meng, J., et al. (2014). Synchronous turnover of flora, fauna and climate at the eocene–oligocene boundary in Asia. *Sci. Rep.* 4, 7463. doi:10.1038/srep07463

Tinner, W., and Hu, F. S. (2003). Size parameters, size-class distribution and area-number relationship of microscopic charcoal: Relevance for fire reconstruction. *Holocene* 13, 499–505. doi:10.1191/0959683603hl615rp

Wang, S., Li, R., Wu, Y., and Zhao, S. (2022). Effects of multi-temporal scale drought on vegetation dynamics in Inner Mongolia from 1982 to 2015, China. *Ecol. Indic.* 136, 108666. doi:10.1016/j.ecolind.2022.108666

Wang, Y., Meng, J., Beard, C. K., Li, Q., Ni, X., Gebo, D. L., et al. (2010). Early Paleogene stratigraphic sequences, mammalian evolution and its response to environmental changes in Erlian Basin, Inner Mongolia, China. *Sci. China Earth Sci.* 53, 1918–1926. doi:10.1007/s11430-010-4095-8

Wang, Y. Q., Meng, J., Jin, X., and Palasiatica, V. (2012). Comments on Paleogene localities and stratigraphy in the Erlian Basin, nei mongol, China. *Vertebr. Palasiat.* 50, 181–203. http://www.vertpala.ac.cn/EN/Y2012/V50/I3/181.

West, C. K., Greenwood, D. R., Reichgelt, T., Lowe, A. J., Vachon, J. M., and Basinger, J. F. (2020). Paleobotanical proxies for early Eocene climates and ecosystems in northern North America from middle to high latitudes. *Clim. Past.* 16, 1387–1410. doi:10.5194/cp-16-1387-2020

Zachos, J., Pagani, M., Sloan, L., Thomas, E., and Billups, K. (2001). Trends, rhythms, and aberrations in global climate 65 Ma to present. *Science* 292, 686–693. doi:10.1126/science.1059412

Zhang, Z., Flatøy, F., Wang, H., Bethke, I., Bentsen, M., and Guo, Z. (2012). Early Eocene Asian climate dominated by desert and steppe with limited monsoons. *J. Asian Earth Sci.* 44, 24–35. doi:10.1016/j.jseaes.2011.05.013